

Formation of Divalent Ruthenacycles via Oxidative Cyclization of 1,3,5-Cyclooctatriene with Maleic Anhydride or Maleimides: An Intermediate for the Transition Metal-Mediated [6 + 2] Cycloaddition of 1,3,5-Trienes and Alkenes

Yasuyuki Ura,* Taka-aki Utsumi, Hiroshi Tsujita, Kenji Wada, Teruyuki Kondo, and Take-aki Mitsudo*

Department of Energy and Hydrocarbon Chemistry, Graduate School of Engineering, Kyoto University, Nishikyo-ku, Kyoto 615-8510, Japan

Received March 16, 2006

Reactions of a zerovalent ruthenium complex, Ru(η^4 -cod)(η^6 -cot) (**3**; cod = 1,5-cyclooctadiene, cot = 1,3,5-cyclooctatriene), with maleic anhydride or maleimides under mild reaction conditions afforded a series of novel divalent ruthenacycles **4** with an η^5 -cyclooctadienyl moiety via oxidative cyclization between the carbon–carbon double bonds of cot and the electron-deficient alkene. The solid-state structure clearly showed a newly constructed ruthenacycle skeleton, which was formed in a *trans* manner. Complex **4** was further reacted with H₂ and HCl to give hydrogenated and protonated succinimides with a C₈-ring, respectively. When **4** was heated in toluene, a [6 + 2] cycloadduct of cot and a maleimide was obtained via reductive elimination, which shows that a ruthenium-mediated stepwise [6 + 2] cycloaddition was achieved. The addition of PPh₃ to complex **4d** promoted the reductive elimination, while bidentate phosphines such as 1,2-bis(diphenylphosphino)ethane did not give the cycloadduct and stable ruthenacycles **11** were formed instead. Reactions of **4** with CO gave novel tricarbonyl ruthenacycles **12** along with dissociation of the cod ligand, where neither reductive elimination nor CO insertion took place. The results of a theoretical study were consistent with the idea that the energy barriers for reductive elimination from ruthenacycles bearing cod or monophosphine ligands were lower than those from a ruthenacycle bearing a diphosphine ligand. The formation of **12** was found to be more energetically favorable than reductive elimination.

Introduction

Transition metal-mediated or -catalyzed cycloadditions are versatile tools for the synthesis of a wide variety of cyclic compounds through the simultaneous formation of two or more carbon–carbon and/or carbon–heteroatom bonds.¹ Since the Fe-mediated [6 + 2] cycloaddition of 1,3,5-cycloheptatriene with cyclobutenes or alkynes was reported by Pettit et al. (eq 1),² several stoichiometric and catalytic [6 + 2] cycloadditions of conjugated cyclic trienes with alkenes, dienes, and alkynes using several transition metal complexes under either photoirradiated or thermal conditions have been intensively investigated (eq 2).^{3–8} In some cases the reactions were applied to the synthesis of natural products.^{4f,h,9} In contrast to the successful development of catalytic reactions, little effort has been devoted to isolation of the reaction intermediates and investigation of their reactivity.

* To whom correspondence should be addressed. E-mail: yura@scl.kyoto-u.ac.jp; mitsudo@scl.kyoto-u.ac.jp.

(1) (a) Weissrermel, K.; Arpe, H.-J. *Industrial Organic Chemistry*, 4th ed.; VCH: Weinheim, 2000. (b) Cornils, B.; Herrmann, W. A., Eds. *Applied Homogeneous Catalysis with Organometallic Compounds*, 2nd ed.; Wiley-VCH: Weinheim, 2002; Vols. 1–3. (c) Schore, N. E. *Chem. Rev.* **1988**, *88*, 1081. (d) Lautens, M.; Klute, W.; Tam, W. *Chem. Rev.* **1996**, *96*, 49. (e) Frühauf, H. W. *Chem. Rev.* **1997**, *97*, 523.

(2) (a) Ward, J. S.; Pettit, R. *J. Am. Chem. Soc.* **1971**, *93*, 262. (b) Davis, R. E.; Dodds, T. A.; Hseu, T.-H.; Wagnon, J. C.; Devon, T.; Tancrede, J.; McKennis, J. S.; Pettit, R. *J. Am. Chem. Soc.* **1974**, *96*, 7562.

(3) Ti-catalyzed reactions: (a) Mach, K.; Antropiusová, H.; Sedmera, P.; Hanuš, V.; Tureček, F. *J. Chem. Soc., Chem. Commun.* **1983**, 805. (b) Mach, K.; Antropiusová, H.; Petrusová, L.; Hanuš, V.; Tureček, F.; Sedmera, P. *Tetrahedron* **1984**, *40*, 3295. (c) Klein, R.; Sedmera, P.; Čejka, J.; Mach, K. *J. Organomet. Chem.* **1992**, *436*, 143.

Proposed mechanisms for metal-mediated or -catalyzed [6 + 2] cycloaddition are often discussed based on the results of [6

(4) Cr-mediated or -catalyzed reactions: (a) Kreiter, C. G.; Michels, E.; Kurz, H. *J. Organomet. Chem.* **1982**, *232*, 249. (b) Rigby, J. H.; Hensilwood, J. A. *J. Am. Chem. Soc.* **1991**, *113*, 5122. (c) Fischler, I.; Grevels, F.-W.; Leitich, J.; Özkar, S. *Chem. Ber.* **1991**, *124*, 2857. (d) Rigby, J. H.; Short, K. M.; Ateeq, H. S.; Hensilwood, J. A. *J. Org. Chem.* **1992**, *57*, 5290. (e) Chaffee, K.; Sheridan, J. B.; Aistars, A. *Organometallics* **1992**, *11*, 18. (f) Rigby, J. H.; Ateeq, H. S.; Charles, N. R.; Hensilwood, J. A.; Short, K. M.; Sugathapala, P. M. *Tetrahedron Lett.* **1993**, *34*, 5495. (g) Rigby, J. H.; Sandanayaka, V. P. *Tetrahedron Lett.* **1993**, *34*, 935. (h) Rigby, J. H. *Acc. Chem. Res.* **1993**, *26*, 579. (i) Rigby, J. H.; Ahmed, G.; Ferguson, M. D. *Tetrahedron Lett.* **1993**, *34*, 5397. (j) Rigby, J. H.; Pigge, F. C.; Ferguson, M. D. *Tetrahedron Lett.* **1994**, *35*, 8131. (k) Rigby, J. H.; Scribner, S.; Heeg, M. J. *Tetrahedron Lett.* **1995**, *36*, 8569. (l) Chaffee, K.; Huo, P.; Sheridan, J. B.; Barbieri, A.; Aistars, A.; Lalancette, R. A.; Ostrander, R. L.; Rheingold, A. L. *J. Am. Chem. Soc.* **1995**, *117*, 1900. (m) Rigby, J. H.; Sugathapala, P.; Heeg, M. J. *J. Am. Chem. Soc.* **1995**, *117*, 8851. (n) Rigby, J. H.; Kirova-Snover, M. *Tetrahedron Lett.* **1997**, *38*, 8153. (o) Rigby, J. H. *Tetrahedron* **1999**, *55*, 4521. (p) Rigby, J. H.; Kondratenko, M. A.; Fiedler, C. *Org. Lett.* **2000**, *2*, 3917. (q) Rigby, J. H.; Mann, L. W.; Myers, B. J. *Tetrahedron Lett.* **2001**, *42*, 8773. (r) Kündig, E. P.; Rivbivieux, F.; Kondratenko, M. *Synthesis* **2002**, *14*, 2053.

(5) Mo-mediated or -catalyzed reactions: (a) Bourner, D. G.; Brammer, L.; Green, M.; Moran, G.; Orpen, A. G.; Reeve, C.; Schaverien, C. J. *J. Chem. Soc., Chem. Commun.* **1985**, 1409. (b) Schmidt, T.; Bienewald, F.; Goddard, R. J. *Chem. Soc., Chem. Commun.* **1994**, 1857.

(6) Fe-mediated reactions: (a) See ref 2. (b) Green, M.; Heathcock, S. M.; Turney, T. W.; Mingos, D. M. P. *J. Chem. Soc., Dalton Trans.* **1977**, 204.

(7) Ru-mediated reactions: (a) See ref 6b. (b) Itoh, K.; Mukai, K.; Nagashima, H.; Nishiyama, H. *Chem. Lett.* **1983**, 499. (c) Nagashima, H.; Matsuda, H.; Itoh, K. *J. Organomet. Chem.* **1983**, *258*, C15.

(8) Co-catalyzed reaction: Achard, M.; Tenaglia, A.; Buono, G. *Org. Lett.* **2005**, *7*, 2353.

(9) Rigby, J. H.; Pigge, F. C. *J. Org. Chem.* **1995**, *60*, 7392.

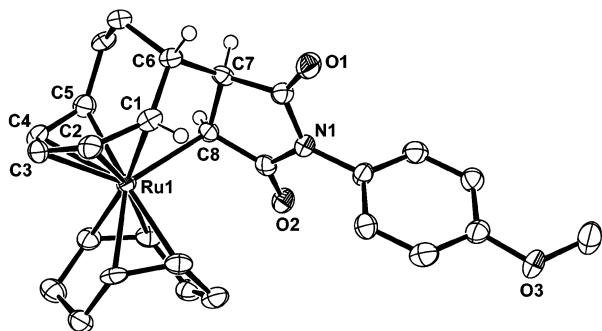


Figure 1. ORTEP drawing of **4e**. Thermal ellipsoids are shown at the 50% probability level. Hydrogen atoms are omitted for clarity except for those on C1, C6, C7, and C8. Selected bond distances (Å): Ru1–C1 = 2.228(5), Ru1–C2 = 2.200(5), Ru1–C3 = 2.250(5), Ru1–C4 = 2.227(5), Ru1–C5 = 2.224(5), Ru1–C8 = 2.266(5), C1–C2 = 1.381(8), C1–C6 = 1.504(7), C2–C3 = 1.440(8), C3–C4 = 1.400(8), C4–C5 = 1.420(7), C6–C7 = 1.524(7), C7–C8 = 1.547(7).

Single crystals of **4e** were obtained by recrystallization from $\text{CHCl}_3/\text{pentane}$, and the molecular structure was determined by X-ray crystallography (Figure 1). A new C–C bond was formed between C6 and C7 in a *trans* manner. The bond distances of C1–C6, C6–C7, and C7–C8 are in the range of C–C single bonds (1.504(7), 1.524(7), and 1.547(7) Å, respectively). The average Ru–C bond distance in the η^5 -cyclooctadienyl moiety is 2.23 Å, which is slightly shorter than the Ru1–C8 bond distance of 2.266(5) Å. The five-membered ring (Ru1–C1–C6–C7–C8) clearly corresponds to a newly constructed ruthenacyclopentane skeleton.

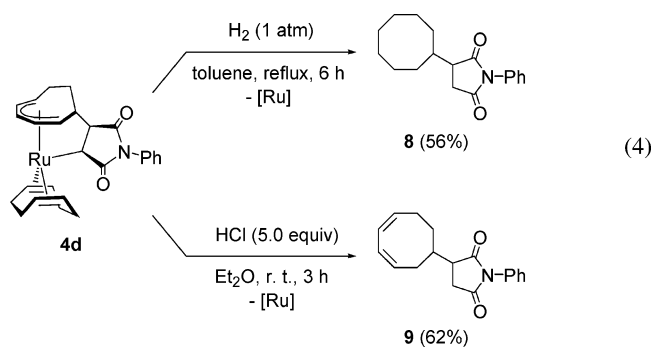
In the ^1H NMR spectra of **4**, the methyne protons of the η^5 -moiety were observed within a wide range, at 2.6–6.6 ppm, while those of cod appeared within a rather narrow range, at 2.8–3.9 ppm. The signal for the α -hydrogen on the sp^3 carbon (corresponding to H on C8 in Figure 1) appeared as a doublet at 4.2–4.4 ppm. The β -hydrogen signal (H on C7) also appeared as a doublet, which was not split by the H on C6 (e.g., the dihedral angle of H–C6–C7–H in **4e** is ca. 80°). In the ^{13}C NMR spectra of **4**, the coordinated carbons of the cyclooctadienyl moiety and cod appeared at a higher magnetic field, at 62–106 and 76–93 ppm, respectively. The sp^3 α -carbon signal (C8) had almost the same chemical shifts (29–35 ppm) as that of free succinic anhydride or succinimides, while the sp^3 β -carbon signal (C7) was shifted to a lower field by ca. 30 ppm.

Other electron-deficient alkenes were also examined in addition to maleic anhydride and maleimides. The reaction of **3** with dimethyl fumarate or dimethyl maleate afforded the zerovalent complex $\text{Ru}(\eta^6\text{-cot})(\eta^2\text{-dimethyl fumarate})_2$.^{12b}

p-Benzoquinone gave an insoluble material that could not be characterized by usual analytical methods.^{12c} Methyl acrylate, *N,N*-dimethylacrylamide, and methyl vinyl ketone were also used; however, almost no reaction proceeded, even at higher temperature, and **3** remained unreacted, probably due to their relatively poor electron-accepting abilities. On the other hand, the reaction of **3** with terminal alkynes has been reported, where [6 + 2] cycloaddition of cot and alkynes proceeded to give zerovalent complexes with a resulting η^4, η^2 -bicyclodecatriene ligand.^{7b}

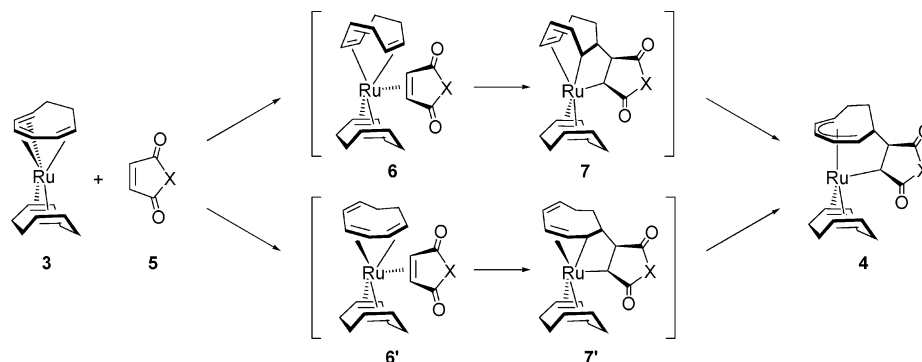
Possible pathways for the formation of **4** are depicted in Scheme 1. The coordination mode of the cot ligand in **3** initially changes from 1-6- η^6 to either 1-2:5-6- η^4 or 1-4- η^4 , and then **5** occupies the vacant coordination site to give **6** or **6'**. It is known that cot is more labile than cod in **3** to afford $\text{Ru}(\eta^4\text{-cod})(\eta^4\text{-cot})(\text{L})$ (L = monodentate ligand), by the reaction of **3** with either CO ^{15b} or phosphorus ligands.^{15d,17a} Oxidative cyclization between C=C of cot and **5** gives coordinatively unsaturated 16e ruthenacyclopentane intermediate **7** or **7'**, and subsequent recoordination of the dissociated C=C leads to ruthenacycles **4** with an η^5 -cyclooctadienyl moiety. Complexes **4** are rare examples of isolated ruthenacycles formed via oxidative cyclization of carbon–carbon double bonds.³³

Reactivity of Ruthenacycles 4: (a) Hydrogenation and Protonolysis. To investigate the fundamental reactivity of the ruthenacycles, hydrogenation and protonolysis of **4d** were performed (eq 4). When **4d** was reacted with H_2 at 1 atm, *N*-phenylcyclooctylsuccinimide **8** was obtained in 56% isolated yield. On the other hand, treatment with HCl in Et_2O afforded *N*-phenyl(3,5-cyclooctadien-1-yl)succinimide **9** in 62% yield under mild reaction conditions. In this reaction, selective protonolysis of the η^5 -cyclooctadienyl moiety occurred at the 2-position and no other isomers were observed at all.



(b) Ruthenium-Mediated Stepwise [6 + 2] Cycloaddition of 1,3,5-Cyclooctatriene and Phenylmaleimide. When **4d** was heated at 50 °C in toluene in the presence or absence of PPh_3 , ring-closure of the ruthenacycle moiety proceeded to give

Scheme 1. Possible Pathways for the Formation of **4**



tricyclic product **10**, and this involved reductive elimination between the carbon atoms corresponding to C5 and C8 in Figure 1 (eq 5, Table 1). Without PPh₃, the reaction proceeded slowly to afford **10** in 6% and 18% yield after 1 h and 18 h, respectively (runs 1 and 2). As shown in runs 3–6, addition of PPh₃ facilitated the reductive elimination, and the use of 3.0 equiv of PPh₃ gave the product in 31% yield even after 1 h (run 5). In all cases, only the *endo*-isomer was obtained, which reflects retention of the steric structure in **4d**. The product **10** can be regarded as a [6 + 2] cycloadduct of a cot ligand and *N*-phenylmaleimide. ¹H NMR analysis of a toluene-*d*₃ solution of **4d** that was heated at 50 °C for 18 h indicated that **4d** was almost converted and several new complexes as well as **10** seemed to be formed concurrently. One of the formed complexes was expected to have **10** as a ligand; however, attempts to isolate the complexes were unsuccessful, probably due to their instability.

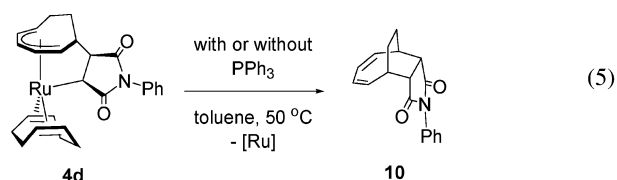


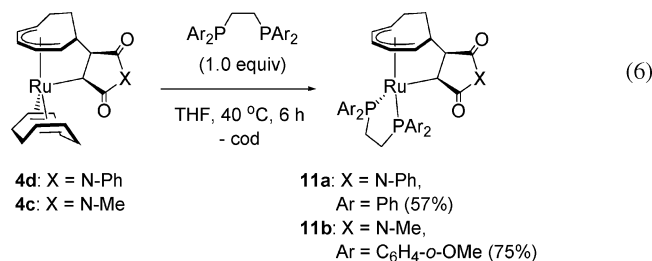
Table 1. Effect of PPh₃ on the Formation of 10 from 4d

run	PPh ₃ (equiv)	time/h	yield/% ^a
1		1	6
2		18	18
3	1.0	1	14
4	2.0	1	18
5	3.0	1	31
6	5.0	1	26

^a NMR yield.

(c) Reaction of 4 with Bidentate Phosphorus Ligands.

Since the addition of PPh₃ was found to accelerate the formation of **10** from **4d**, 1,2-bis(diphenylphosphino)ethane (dppe) was also used as an additive. However, no **10** was formed in this case. Instead, a novel ruthenacycle **11a** bearing dppe was obtained, as shown in eq 6, via ligand displacement between cod and dppe. The reaction of **4c** with 1,2-bis(di(*o*-methoxyphenyl)phosphino)ethane gave a similar complex **11b** in good yield. Fine pale yellow single crystals of **11a** were obtained by recrystallization from CH₂Cl₂/pentane, and the X-ray structure is shown in Figure 2.



When **11a** was heated to 50 °C in toluene for 24 h, no formation of **10** occurred and **11a** remained unreacted. This is in contrast to the results with the monodentate phosphine PPh₃. We believe that if more than 2 equiv of PPh₃ are added to **4d**,

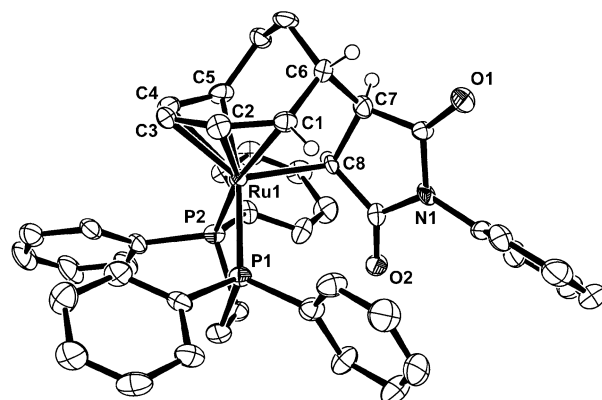


Figure 2. ORTEP drawing of **11a**. Thermal ellipsoids are shown at the 50% probability level. Solvent molecules and hydrogen atoms are omitted for clarity except for those on C1, C6, C7, and C8. Selected bond distances (Å): Ru1–P1 = 2.3282(15), Ru1–P2 = 2.3110(17), Ru1–C1 = 2.226(6), Ru1–C2 = 2.211(6), Ru1–C3 = 2.247(6), Ru1–C4 = 2.202(6), Ru1–C5 = 2.219(6), Ru1–C8 = 2.212(5), C1–C2 = 1.405(8), C1–C6 = 1.530(7), C2–C3 = 1.435(9), C3–C4 = 1.408(10), C4–C5 = 1.416(8), C6–C7 = 1.550(8), C7–C8 = 1.563(8).

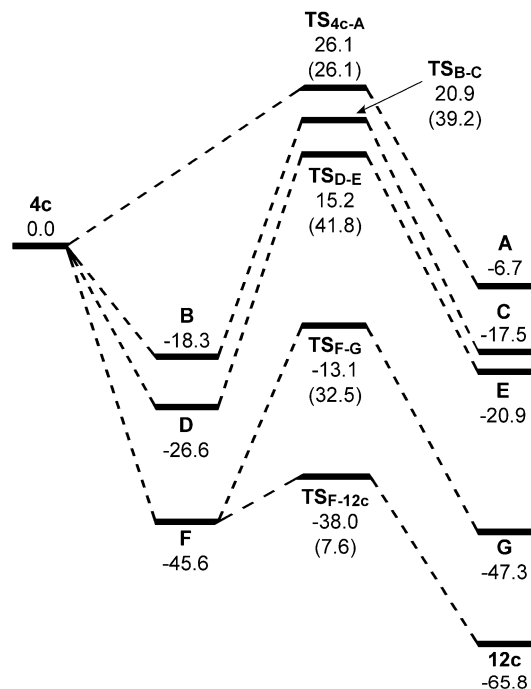
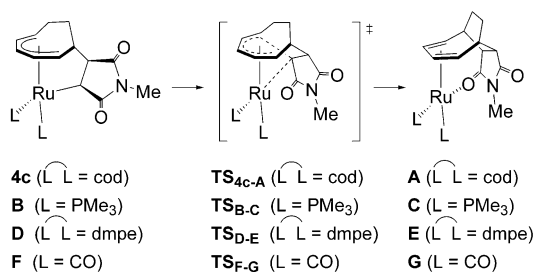


Figure 3. Energy profile for reductive elimination from **4c**, **B**, **D**, and **F** to **A**, **C**, **E**, and **G**, and for the formation of tricarbonyl complex **12c** from **F**. The values in parentheses show net activation energies for the respective steps.

the cod ligand would be replaced to form a bis-PPh₃ ruthenacycle complex, where the steric constraints between PPh₃ and the ruthenacycle moiety would be greater than those in complex **11**, which would facilitate reductive elimination.

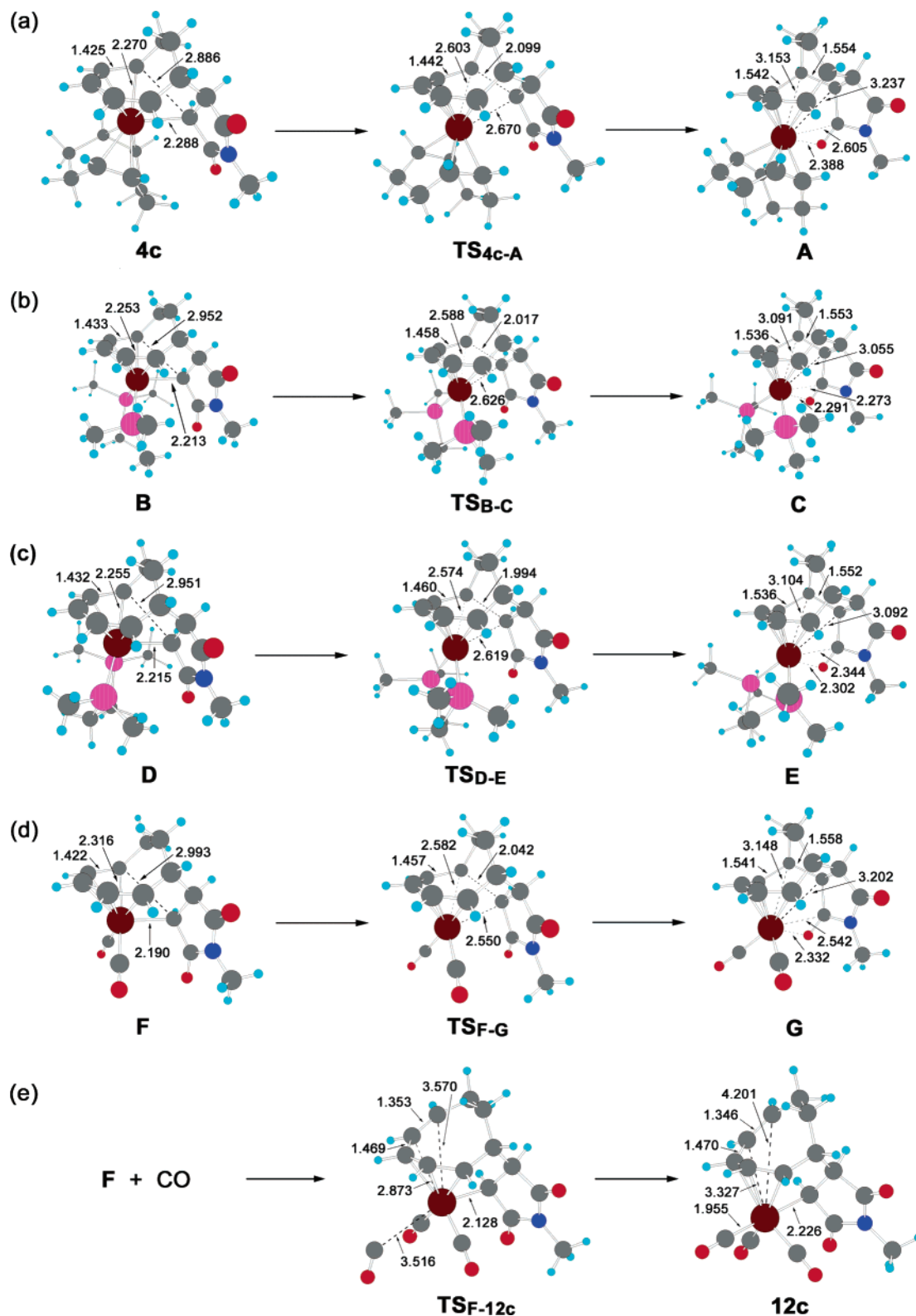
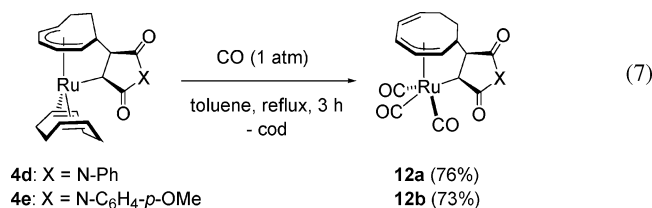


Figure 4. Optimized structures of (a) **4c**, **TS_{4c-A}**, and **A**, (b) **B**, **TS_{B-C}**, and **C**, (c) **D**, **TS_{D-E}**, and **E**, (d) **F**, **TS_{F-G}**, and **G**, and (e) **TS_{F-12c}** and **12c**. Selected atomic distances (Å) are shown in each structure.

(d) Reaction of 4 with CO. The reaction of **4** with CO was also investigated with the expectation of either promoting reductive elimination or effecting CO insertion into the ruthenacycle. Complexes **4d** and **4e** were treated under CO at 1 atm in toluene and refluxed for 3 h to give tricarbonyl ruthenacycle complexes **12a** in 76% yield and **12b** in 73% yield, respectively (eq 7). In these reactions, cod was fully dissociated

and instead three molecules of CO coordinated to Ru, along with a change in the hapticity of the cyclooctadienyl moiety from η^5 to η^3 . The free double-bond moiety of the C₈-ring appeared characteristically in the ¹³C NMR spectra at 132.4 and 133.4 ppm and at 129.3 and 132.4 ppm for **12a** and **12b**, while the coordinated carbon atoms of the C₈-ring are normally observed in the range 50–110 ppm. Treatment of **4e** under more

severe reaction conditions such as CO at 40 atm and 120 °C also afforded only **12b**, and products derived from either reductive elimination or CO insertion were not obtained at all.



Density Functional Study. The reductive elimination step from ruthenacycles was investigated theoretically by the DFT method. As depicted in the upper part of Figure 3, complexes **4c**, **B**, **D**, and **F** were used as starting complexes. **B** is a model intermediate in the reaction described in eq 5 in the presence of PPh₃, and **D** is a model complex of **11**. Dicarboxyl complex **F**, which can be regarded as an intermediate in the formation of tricarbonyl complex **12c** (X = NMe), was also investigated for comparison. **A**, **C**, **E**, and **G** are corresponding zerovalent diene complexes formed via reductive elimination from **4c**, **B**, **D**, and **F**, respectively. The geometries of the stable complexes **4c**, **A–G**, and **12c** and transition states **TS**_{4c–A}, **TS**_{B–C}, **TS**_{D–E}, **TS**_{F–G}, and **TS**_{F–12c} were optimized by the B3LYP method with a basis set composed of the combination of SDD for Ru and 6-31G(d,p) for all other atoms. The energy profile (ΔE_0) is shown in the lower part of Figure 3, and the optimized structures are shown in Figure 4.

The ligand displacement of cod in **4c** with PMe₃, dmpe, or CO is thermodynamically favorable. The energy barrier of **TS**_{4c–A} is 26.1 kcal/mol, which was lower than those of **TS**_{B–C}, **TS**_{D–E}, and **TS**_{F–G}. In **TS**_{4c–A}, the bond distances between Ru and two carbon atoms (corresponding to C5 and C8 in Figure 1) increase from 2.270 and 2.288 to 2.603 and 2.670 Å, and the distance between these carbon atoms shortens from 2.886 to 2.099 Å. The geometry of **A** reveals that a new C–C single bond is formed to build a tricyclic skeleton, and one of the carbonyl groups of the succinimide moiety has weak interaction with Ru to occupy the vacant coordination site, to form a twisted structure. In **B** and **D**, the bond angles of P–Ru–P are 94.511° and 83.365°, respectively, which reflects the steric difference. The energy barrier for reductive elimination from bis-mono-phosphine complex **B** (39.2 kcal/mol) is slightly lower than that from diphosphine complex **D** (41.8 kcal/mol). This difference is consistent with the experimental results, where PPh₃ and dppe correspond to mono- and diphosphine, respectively. The barrier of **TS**_{F–G} was estimated to be 32.5 kcal/mol, which is lower than those of **TS**_{B–C} and **TS**_{D–E}. However, there is an alternative, almost spontaneous, pathway from **F** to tricarbonyl complex **12c** via **TS**_{F–12c}, and this is also consistent with the experimental results shown in eq 7, where reductive elimination did not take place. In **TS**_{F–12c}, the hapticity of the cyclooctadienyl moiety is already converted from η^5 to η^3 , and it has a structure that is partially similar to that in **12c**.

As expected, CO was revealed to have a greater ability to stabilize the divalent ruthenacycle species than cod, PMe₃, or dmpe. It is generally accepted that reductive elimination is facilitated by strong π -accepting ligands such as CO. However, in our system, **TS**_{4c–A} and **TS**_{F–G} showed an opposite order of the energy barrier. This result can be explained by steric factors; that is, in **TS**_{4c–A}, the steric hindrance of the ruthenacycle moiety against cod is greater than that against CO in **TS**_{F–G}, and overall reductive elimination from **4c** has a lower barrier than that from **F**.

The relatively greater steric hindrance of the ruthenacycle moiety against PMe₃ in **TS**_{B–C} compared to that against dmpe in **TS**_{D–E} may explain the difference in energy barriers in the reductive elimination process. Note that, in the experiment, more bulky and π -accepting phosphine ligands than PMe₃ or dmpe were used, which would further lower the energy barriers for the reductive elimination of these complexes in comparison with the model complexes. The experimental results in eq 5 indicate that the energy barrier for reductive elimination from the bis-PPh₃ ruthenacycle complex may be even lower than that from **4c**, whereas PPh₃ might also promote dissociation of the formed [6 + 2] cycloadduct from ruthenium.

Conclusion

The synthesis, structure, and reactivity of novel ruthenacycles formed via oxidative cyclization of carbon–carbon double-bond moieties of 1,3,5-cyclooctatriene and maleic anhydride or maleimides were reported. These ruthenacycles were shown to be intermediates in transition metal-mediated [6 + 2] cycloaddition, and the cycloaddition could be performed in a stepwise manner. The spectator ligands were experimentally shown to have significant steric and electronic effects upon reductive elimination from the ruthenacycles, and moreover, the results were supported theoretically by DFT calculation. These findings may contribute to the further understanding of metal-mediated or -catalyzed [6 + 2] cycloaddition and to the development of novel catalytic transformation reactions via metallacycle intermediates.

Experimental Section

Materials and Methods. All manipulations were performed under an argon atmosphere using standard Schlenk techniques. All solvents were distilled under argon over appropriate drying reagents (sodium, calcium hydride, sodium benzophenoneketyl, or calcium chloride). Ru(η^4 -cod)(η^6 -cot) (**3**)^{15c,21} and *N-p*-methoxyphenylmaleimide³⁴ were prepared as reported in the literature.

Physical and Analytical Measurements. NMR spectra were recorded on JEOL EX-400 (FT, 400 MHz (¹H), 100 MHz (¹³C)) and AL-300 (FT, 300 MHz (¹H), 75 MHz (¹³C)) spectrometers. Chemical shift values (δ) for ¹H and ¹³C are referenced to internal solvent resonances and reported relative to SiMe₄. IR spectra were recorded on a Nicolet Impact 410 FT-IR spectrometer. Melting points were measured under argon on a Yanagimoto micro melting point apparatus.

Synthesis of Ruthenacycles 4a–e. Ruthenacycles **4a–e** were synthesized in a similar manner. The following procedure for **4a** is representative.

Complex 4a. Into a 20 mL, two-necked Pyrex flask with a stirring bar were placed complex **3** (221 mg, 0.70 mmol) and maleic anhydride (69 mg, 0.70 mmol) under an argon atmosphere. Hexane (5.0 mL) was then added, and the suspension was magnetically stirred at 40 °C for 2 h. The resulting pale yellow precipitate was filtered by a G4-glass filter, washed three times with 3 mL of Et₂O, and dried under vacuum to give the title complex **4a** (194 mg, 67%) as a pale yellow solid. Mp: 144–146 °C (dec). IR (KBr disk): 1993, 1802, 1739, 1237, 1221 cm⁻¹. ¹H NMR (400 MHz, CD₂-Cl₂): δ 6.60 (t, *J* = 7.3 Hz, 1H, CH of cyclooctadienyl), 5.10 (t, *J* = 8.5 Hz, 1H, CH of cyclooctadienyl), 4.28 (d, *J* = 4.8 Hz, 1H, CH of cyclooctadienyl), 4.25 (d, *J* = 5.2 Hz, 1H, RuCH), 4.06 (dd, *J* = 10.4, 6.4 Hz, 1H, CH of cyclooctadienyl), 3.81 (d, *J* = 7.2 Hz, 1H, RuCHCH), 3.59–3.55 (m, 2H, CH of cod), 3.18 (dt, *J* = 4.7, 7.9 Hz, 1H, CH of cod), 3.03 (ddd, *J* = 2.1, 6.7, 8.7 Hz, 1H, CH of cod), 3.04 (t, *J* = 6.6 Hz, 1H, CH of cyclooctadienyl),

2.72–2.56 (m, 3H, CH₂ of cod and CH of cyclooctadienyl), 2.14–2.04 (m, 2H, CH₂ of cod), 1.95–1.80 (m, 4H, CH₂ of cod and cyclooctadienyl), 1.72 (ddt, $J = 16.1, 14.2, 4.7$ Hz, 1H, CH₂ of cyclooctadienyl), 1.64–1.57 (m, 1H, CH₂ of cod), 1.13–1.09 (m, 1H, CH₂ of cyclooctadienyl), 0.41 (dt, $J = 4.9, 14.2$ Hz, 1H, CH₂ of cyclooctadienyl). ¹³C NMR (100 MHz, CD₂Cl₂): δ 183.5 (C=O), 178.3 (C=O), 106.3 (CH of cyclooctadienyl), 101.5 (CH of cyclooctadienyl), 99.6 (CH of cyclooctadienyl), 92.1 (CH of cod), 88.5 (CH of cod), 86.6 (CH of cyclooctadienyl), 81.9 (CH of cod), 78.9 (CH of cod), 64.6 (RuCHCH), 64.4 (CH of cyclooctadienyl), 41.7 (CH of cyclooctadienyl), 34.7 (CH₂ of cod), 33.3 (CH₂ of cod), 29.8 (RuCH), 29.6 (CH₂ of cod), 28.6 (CH₂ of cod), 23.5 (CH₂ of cyclooctadienyl), 23.1 (CH₂ of cyclooctadienyl). HR-MS (FAB-*m*NBA): calcd for C₂₀H₂₃O₃Ru 413.0691, found 413.0682 (M⁺ – H).

Complex 4b: pale yellow solid, mp 126–128 °C (dec). IR (KBr disk): 3146, 1720, 1673, 1446, 1347, 1172 cm⁻¹. ¹H NMR (400 MHz, CDCl₃): δ 8.12 (br s, NH), 6.53 (t, $J = 7.1$ Hz, 1H, CH of cyclooctadienyl), 5.12 (t, $J = 8.5$ Hz, 1H, CH of cyclooctadienyl), 4.19 (d, $J = 6.8$ Hz, 1H, RuCH), 4.13 (d, $J = 4.9$ Hz, 2H, CH of cyclooctadienyl), 3.83 (dt, $J = 4.6, 8.4$ Hz, 1H, CH of cod), 3.78 (d, $J = 6.3$ Hz, 1H, RuCHCH), 3.58 (br t, $J = 6.1$ Hz, 1H, CH of cod), 3.18–3.13 (m, 2H, CH of cyclooctadienyl and cod), 2.97 (t, $J = 7.3$ Hz, 1H, CH of cod), 2.85–2.63 (m, 3H, CH₂ of cod and CH of cyclooctadienyl), 2.29–2.19 (m, 1H, CH₂ of cod), 2.04 (br t, $J = 11.6$ Hz, 1H, CH₂ of cod), 1.97–1.76 (m, 5H, CH₂ of cyclooctadienyl and cod), 1.65–1.57 (m, 1H, CH₂ of cod), 1.21–1.14 (m, 1H, CH₂ of cyclooctadienyl), 0.50 (dt, $J = 5.2, 14.0$ Hz, 1H, CH₂ of cyclooctadienyl). ¹³C NMR (100 MHz, CDCl₃): δ 190.9 (C=O), 181.6 (C=O), 105.0 (CH of cyclooctadienyl), 100.9 (CH of cyclooctadienyl), 99.6 (CH of cyclooctadienyl), 92.6 (CH of cod), 89.5 (CH of cod), 87.8 (CH of cyclooctadienyl), 79.5 (CH of cod), 76.7 (CH of cod), 65.6 (RuCHCH), 62.4 (CH of cyclooctadienyl), 39.8 (CH of cyclooctadienyl), 35.4 (CH₂ of cod), 34.7 (RuCH), 32.2 (CH₂ of cod), 30.5 (CH₂ of cod), 28.6 (CH₂ of cod), 23.2 (CH₂ of cyclooctadienyl), 23.1 (CH₂ of cyclooctadienyl). HR-MS (FAB-*m*NBA): calcd for C₂₀H₂₄NO₂Ru 412.0851, found 412.0831 (M⁺ – H).

Complex 4c: pale yellow solid, mp 129–132 °C (dec). IR (KBr disk): 1729, 1663, 1439, 1383, 1267 cm⁻¹. ¹H NMR (400 MHz, CD₂Cl₂): δ 6.51 (dd, $J = 8.3, 6.8$ Hz, 1H, CH of cyclooctadienyl), 5.10 (t, $J = 8.3$ Hz, 1H, CH of cyclooctadienyl), 4.18 (d, $J = 6.8$ Hz, 1H, RuCH), 4.10 (dd, $J = 6.8, 10.3$ Hz, 1H, CH of cyclooctadienyl), 4.02 (dd, $J = 6.3, 10.3$ Hz, 1H, CH of cyclooctadienyl), 3.84 (dt, $J = 4.2, 8.4$ Hz, 1H, CH of cod), 3.65 (d, $J = 6.3$ Hz, 1H, RuCHCH), 3.59–3.53 (m, 1H, CH of cod), 3.23 (s, 3H, NCH₃), 3.19 (t, $J = 6.6$ Hz, 1H, CH of cyclooctadienyl), 3.09 (dd, $J = 8.3, 13.2$ Hz, 1H, CH of cod), 2.89–2.79 (m, 2H, CH and CH₂ of cod), 2.64–2.54 (m, 2H, CH of cyclooctadienyl and CH₂ of cod), 2.26–2.17 (m, 2H, CH₂ of cod), 2.01 (br t, $J = 12.0$ Hz, 1H, CH₂ of cod), 1.94–1.80 (m, 4H, CH₂ of cyclooctadienyl and cod), 1.66–1.57 (m, 1H, CH₂ of cod), 1.25–1.13 (m, 1H, CH₂ of cyclooctadienyl), 0.50 (dt, $J = 6.0, 13.6$ Hz, 1H, CH₂ of cyclooctadienyl). ¹³C NMR (100 MHz, CD₂Cl₂): δ 191.0 (C=O), 181.1 (C=O), 105.0 (CH of cyclooctadienyl), 100.9 (CH of cyclooctadienyl), 99.7 (CH of cyclooctadienyl), 92.2 (CH of cod), 89.1 (CH of cod), 87.1 (CH of cyclooctadienyl), 79.3 (CH of cod), 76.8 (CH of cod), 64.3 (RuCHCH), 62.5 (CH of cyclooctadienyl), 39.7 (CH of cyclooctadienyl), 35.2 (CH₂ of cod), 33.7 (RuCH), 32.2 (CH₂ of cod), 30.8 (CH₂ of cod), 28.5 (CH₂ of cod), 24.6 (NCH₃), 23.2 (CH₂ of cyclooctadienyl), 23.2 (CH₂ of cyclooctadienyl). HR-MS (FAB-*m*NBA): calcd for C₂₁H₂₆NO₂Ru 426.1007, found 426.0995 (M⁺ – H).

Complex 4d: pale yellow solid, mp 129–134 °C (dec). IR (KBr disk): 1732, 1677, 1499, 1379, 1157 cm⁻¹. ¹H NMR (400 MHz, CD₂Cl₂): δ 7.55–7.33 (m, 5H, H_{Ar}), 6.55 (t, $J = 7.1$ Hz, 1H, CH of cyclooctadienyl), 5.12 (dd, $J = 7.3, 9.3$ Hz, 1H, CH of

cyclooctadienyl), 4.38 (d, $J = 6.8$ Hz, 1H, RuCH), 4.27–4.17 (m, 2H, CH of cyclooctadienyl), 3.88 (dt, $J = 4.4, 8.3$ Hz, 1H, CH of cod), 3.84 (d, $J = 6.3$ Hz, 1H, RuCHCH), 3.60 (dt, $J = 8.8, 4.4$ Hz, 1H, CH of cod), 3.29 (t, $J = 6.3$ Hz, 1H, CH of cod), 3.19–3.10 (m, 2H, CH of cyclooctadienyl and cod), 2.85–2.76 (m, 1H, CH₂ of cod), 2.70 (dt, $J = 9.3, 4.3$ Hz, 1H, CH of cyclooctadienyl), 2.55 (dq, $J = 19.0, 6.9$ Hz, 1H, CH₂ of cod), 2.26–2.21 (m, 2H, CH₂ of cod), 2.00–1.79 (m, 5H, CH₂ of cyclooctadienyl and cod), 1.61–1.52 (m, 1H, CH₂ of cyclooctadienyl), 1.27–1.22 (m, 1H, CH₂ of cod), 0.54 (dt, $J = 6.5, 13.3$ Hz, 1H, CH₂ of cyclooctadienyl). ¹³C NMR (100 MHz, CD₂Cl₂): δ 189.4 (C=O), 180.3 (C=O), 134.1 (C_{Ar}), 128.9 (2C, C_{Ar}), 127.6 (C_{Ar}), 127.1 (2C, C_{Ar}), 105.2 (CH of cyclooctadienyl), 101.1 (CH of cyclooctadienyl), 99.7 (CH of cyclooctadienyl), 92.5 (CH of cod), 89.3 (CH of cod), 87.7 (CH of cyclooctadienyl), 79.5 (CH of cod), 76.8 (CH of cod), 64.3 (CH of cyclooctadienyl), 62.7 (RuCHCH), 40.2 (CH of cyclooctadienyl), 35.2 (CH₂ of cod), 33.2 (RuCH), 32.4 (CH₂ of cod), 30.6 (CH₂ of cod), 28.4 (CH₂ of cod), 23.3 (CH₂ of cyclooctadienyl), 23.2 (CH₂ of cyclooctadienyl). Anal. Calcd for C₂₆H₂₉NO₂Ru: C, 63.91; H, 5.98; N, 2.87. Found: C, 63.75; H, 5.93; N, 3.06.

Complex 4e: pale yellow solid, mp 139–141 °C (dec). IR (KBr disk): 1708, 1676, 1512, 1302, 1250, 1171 cm⁻¹. ¹H NMR (400 MHz, CD₂Cl₂): δ 7.38 (d, $J = 8.8$ Hz, 2H, H_{Ar}), 7.03 (d, $J = 8.8$ Hz, 2H, H_{Ar}), 6.58 (t, $J = 6.8$ Hz, 1H, CH of cyclooctadienyl), 5.15 (t, $J = 8.6$ Hz, 1H, CH of cyclooctadienyl), 4.28 (d, $J = 6.8$ Hz, 1H, RuCH), 4.24–4.17 (m, 2H, CH of cyclooctadienyl), 3.86 (s, 3H, OCH₃), 3.83–3.80 (m, 1H, CH of cod), 3.80 (d, $J = 6.8$ Hz, 1H, RuCHCH), 3.61 (br t, $J = 4.4$ Hz, 1H, CH of cod), 3.22–3.14 (m, 2H, CH of cyclooctadienyl and CH of cod), 3.06 (t, $J = 7.4$ Hz, 1H, CH of cod), 2.75–2.68 (m, 2H, CH of cyclooctadienyl and CH₂ of cod), 2.56–2.46 (m, 1H, CH₂ of cod), 2.26–2.23 (m, 2H, CH₂ of cod), 2.00–1.78 (m, 4H, CH₂ of cyclooctadienyl and CH₂ of cod), 1.53 (br s, 1H, CH₂ of cod), 1.26–1.21 (m, 1H, CH₂ of cyclooctadienyl), 0.55 (dt, $J = 14.0, 9.5$ Hz, 1H, CH₂ of cod). ¹³C NMR (100 MHz, CD₂Cl₂): δ 189.6 (C=O), 180.6 (C=O), 159.1 (C_{Ar}), 128.8 (2C, C_{Ar}), 127.5 (C_{Ar}), 114.3 (2C, C_{Ar}), 105.4 (CH of cyclooctadienyl), 101.5 (CH of cyclooctadienyl), 100.2 (CH of cyclooctadienyl), 92.9 (CH of cod), 89.5 (CH of cod), 88.1 (CH of cyclooctadienyl), 79.5 (CH of cod), 76.6 (CH of cod), 64.7 (RuCHCH), 63.0 (CH of cyclooctadienyl), 55.8 (OCH₃), 40.6 (CH of cyclooctadienyl), 35.5 (CH₂ of cod), 33.7 (RuCH), 32.5 (CH₂ of cod), 30.9 (CH₂ of cod), 28.6 (CH₂ of cod), 23.6 (CH₂ of cyclooctadienyl), 23.5 (CH₂ of cyclooctadienyl). HR-MS (FAB-*m*NBA): calcd for C₂₇H₃₀NO₃Ru 518.1269, found 518.1290 (M⁺ – H).

Synthesis of *N*-Phenylcyclooctylsuccinimide 8. Into a 20 mL, two-necked Pyrex flask with a stirring bar and a reflux condenser was placed **4d** (244 mg, 0.50 mmol) under a H₂ atmosphere. Toluene (5 mL) was then added, and the solution was magnetically stirred at 120 °C for 6 h. The resulting dark brown precipitate was removed by a G4-glass filter, and the filtrate was purified by column chromatography with functionalized silica gel. Removal of solvents gave **8** (80 mg, 56%) as a white solid. Mp: 112–115 °C (dec). IR (KBr disk): 1741, 1689, 1513, 1301, 1250, 1171 cm⁻¹. ¹H NMR (400 MHz, CDCl₃): δ 7.47 (tt, $J = 7.6, 1.5$ Hz, 2H), 7.39 (tt, $J = 7.6, 1.6$ Hz, 1H), 7.27 (dd, $J = 7.6, 1.2$ Hz, 2H), 2.99 (ddd, $J = 9.3, 4.4, 3.4$ Hz, 1H), 2.87 (dd, $J = 18.3, 9.3$ Hz, 1H), 2.63 (dd, $J = 18.3, 4.4$ Hz, 1H), 2.44–2.35 (m, 1H), 1.80–1.41 (m, 14H). ¹³C NMR (100 MHz, CDCl₃): δ 178.6 (C=O), 176.1 (C=O), 132.0, 129.1 (2C), 128.5, 126.4 (2C), 47.1, 37.8, 32.2, 31.2, 28.5, 26.4, 26.3 (2C), 26.0, 25.4. HR-MS (FAB-*m*NBA): calcd for C₁₈H₂₄NO₂ 286.1807, found 286.1810 (M⁺ + H).

Synthesis of *N*-Phenyl(3,5-cyclooctadien-1-yl)succinimide 9. Into a 20 mL, two-necked Pyrex flask with a stirring bar was placed **4d** (146 mg, 0.30 mmol) under an argon atmosphere. Et₂O (1.5 mL) and 1.0 M HCl (Et₂O solution, 1.5 mL) were added, and the suspension was magnetically stirred at room temperature for 3 h.

The resulting pale orange solid was filtered off by a G4-glass filter. The filtrate was chromatographed on silica gel, and elution with Et₂O gave a pale yellow solution, from which the solvent was evaporated to give **9** (52 mg, 62%) as a white solid. Mp: 101–104 °C. IR (KBr disk): 2922, 1779, 1703, 1593, 1501, 1457, 1391, 1262 cm⁻¹. ¹H NMR (400 MHz, CD₂Cl₂): δ 7.50 (t, *J* = 7.2 Hz, 2H), 7.42 (d, *J* = 7.2 Hz, 1H), 7.27 (d, *J* = 7.6 Hz, 2H), 5.91 (d, *J* = 10.8 Hz, 2H), 5.80–5.64 (m, 2H), 3.05 (dt, *J* = 9.3, 4.9 Hz, 1H), 2.87 (dd, *J* = 18.6, 9.3 Hz, 1H), 2.61 (dd, *J* = 18.3, 4.9 Hz, 1H), 2.56–2.38 (m, 1H), 2.29 (br s, 1H), 2.19–2.02 (m, 3H), 1.74 (br t, *J* = 11.7 Hz, 1H), 1.33 (br q, *J* = 11.7 Hz, 1H). ¹³C NMR (100 MHz, CD₂Cl₂): δ 178.5 (C=O), 175.8 (C=O), 132.5 (C_{Ar}), 131.5, 129.8, 129.3 (2C, C_{Ar}), 128.8 (C_{Ar}), 127.2, 126.9 (2C, C_{Ar}), 126.7, 46.1, 35.1, 31.7, 31.3, 28.5, 27.0. HR-MS (FAB-*m*NBA): calcd for C₁₈H₂₀NO₂ 282.1494, found 282.1482 (M⁺ + H).

Formation of 10. Into a 30 mL, two-necked Pyrex flask with a stirring bar was placed **4d** (244 mg, 0.50 mmol) under an argon atmosphere. Toluene (10 mL) was added, and the dark green solution was magnetically stirred at 50 °C for 18 h. The reaction mixture was evaporated, and the residue was purified by silica gel column chromatography (hexane/ethyl acetate, 1:1) to give **10** (18 mg, 13%) as a white solid after drying. Mp: 178–180 °C (dec). IR (KBr disk): 2923, 2854, 1706, 1459, 1377 cm⁻¹. ¹H NMR (300 MHz, CDCl₃): δ 7.45 (tt, *J* = 7.4, 1.5 Hz, 2H), 7.37 (tt, *J* = 7.4, 1.5 Hz, 1H), 7.25 (dd, *J* = 7.4, 1.5 Hz, 2H), 5.81 (dt, *J* = 12.3, 3.5 Hz, 2H), 5.65–5.55 (m, 2H), 3.27 (dt, *J* = 8.4, 6.0 Hz, 2H), 3.13–3.02 (m, 2H), 2.28–2.13 (m, 2H), 1.99–1.83 (m, 2H). ¹³C NMR (75 MHz, CDCl₃): δ 177.4 (2C, C=O), 132.1, 130.8 (2C), 129.0 (2C), 128.4, 126.8 (2C), 126.4 (2C), 44.0 (2C), 31.4 (2C), 25.5 (2C). HR-MS (FAB-*m*NBA): calcd for C₁₈H₁₈NO₂ 280.1338, found 280.1336 (M⁺ + H).

Synthesis of Complexes 11a and 11b. Complexes **11a** and **11b** were synthesized in a similar manner. The following procedure for **11a** is representative.

Complex 11a. Into a 20 mL, two-necked Pyrex flask with a stirring bar were placed complex **4d** (244 mg, 0.50 mmol) and 1,2-bis(diphenylphosphino)ethane (199 mg, 0.50 mmol) under an argon atmosphere. THF (5.0 mL) was then added, and the solution was magnetically stirred at 40 °C for 6 h. The reaction mixture was chromatographed on alumina, and elution with THF gave a yellow solution from which the solvent was evaporated. The resulting yellow solid was reprecipitated from Et₂O/hexane and filtered by a G4-glass filter, washed (4 × 3 mL of hexane), and dried under vacuum to give **11a** (221 mg, 57%): pale yellow solid, mp 150–153 °C (dec). IR (KBr disk): 1723, 1658, 1499, 1432, 1383, 1368, 1156, 1093 cm⁻¹. ¹H NMR (400 MHz, CDCl₃): δ 7.70 (t, *J* = 8.3 Hz, 2H, H_{Ar}), 7.49–7.18 (m, 16H, H_{Ar}), 7.08 (t, *J* = 6.6 Hz, 1H, H_{Ar}), 6.98 (t, *J* = 8.1 Hz, 2H, H_{Ar}), 6.94 (t, *J* = 6.6 Hz, 2H, H_{Ar}), 6.88 (d, *J* = 7.8 Hz, 2H, H_{Ar}), 6.50 (t, *J* = 6.6 Hz, 1H, CH of cyclooctadienyl), 4.87–4.82 (m, 1H, CH of cyclooctadienyl), 4.78 (t, *J* = 8.1 Hz, 1H, CH of cyclooctadienyl), 4.50 (dt, *J* = 8.8, 7.9 Hz, 1H, CH of cyclooctadienyl), 3.75–3.73 (m, 1H, RuCHCH), 3.60 (d, *J* = 7.3 Hz, 1H, RuCH), 3.23–3.03 (m, 2H, CH of cyclooctadienyl and PCH₂), 2.83–2.68 (m, 2H, CH of cyclooctadienyl and PCH₂), 1.90–1.82 (m, 1H, CH₂ of cyclooctadienyl), 1.75–1.65 (m, 1H, CH₂ of cyclooctadienyl), 1.54–1.36 (m, 2H, PCH₂), 1.29–1.26 (m, 1H, CH₂ of cyclooctadienyl), 0.67 (dt, *J* = 4.4, 13.9 Hz, 1H, CH₂ of cyclooctadienyl). ¹³C NMR (100 MHz, CDCl₃): δ 190.6 (C=O), 180.9 (C=O), 140.9–126.1 (C_{Ar}), 99.1 (CH of cyclooctadienyl), 93.2 (d, *J*_{CP} = 2.5 Hz, CH of cyclooctadienyl), 93.1 (s, CH of cyclooctadienyl), 79.0 (d, *J*_{CP} = 17.5 Hz, CH of cyclooctadienyl), 63.9 (d, *J*_{CP} = 8.3 Hz, RuCH), 48.3 (d, *J*_{CP} = 34.2 Hz, CH of cyclooctadienyl), 41.9 (CH of cyclooctadienyl), 29.2 (dd, *J*_{CP} = 30.9, 18.3 Hz, PCH₂), 29.0 (d, *J*_{CP} = 5.8 Hz, RuCHCH), 28.0 (dd, *J*_{CP} = 28.4, 14.2 Hz, PCH₂), 24.8 (CH₂

of cyclooctadienyl), 24.6 (CH₂ of cyclooctadienyl). HR-MS (FAB-*m*NBA): calcd for C₄₄H₄₁NO₂P₂Ru 779.1656, found 779.1669 (M⁺).

Complex 11b: pale yellow solid, mp 145–147 °C (dec). IR (KBr disk): 1725, 1711, 1664, 1650, 1512, 1433, 1298, 1157, 1092 cm⁻¹. ¹H NMR (300 MHz, CD₂Cl₂): δ 8.05 (dt, *J* = 1.5, 7.6 Hz, 1H, H_{Ar}), 7.98 (ddd, *J* = 1.3, 7.5, 13.8 Hz, 1H, H_{Ar}), 7.63 (ddd, *J* = 1.7, 7.3, 14.8 Hz, 1H, H_{Ar}), 7.42 (dt, *J* = 1.0, 8.1 Hz, 1H, H_{Ar}), 7.30 (dt, *J* = 1.3, 7.8 Hz, 1H, H_{Ar}), 7.24–7.14 (m, 3H, H_{Ar}), 7.07 (t, *J* = 7.7 Hz, 1H, H_{Ar}), 7.04 (t, *J* = 7.4 Hz, 2H, H_{Ar}), 6.80–6.68 (m, 3H), 6.69 (t, *J* = 7.2 Hz, 1H, CH of cyclooctadienyl), 6.60 (dd, *J* = 1.7, 8.3 Hz, 1H, H_{Ar}), 6.53 (d, *J* = 8.3 Hz, 1H, H_{Ar}), 5.10–5.03 (m, 1H, CH of cyclooctadienyl), 4.97 (dt, *J* = 8.5, 4.8 Hz, 1H, CH of cyclooctadienyl), 4.32 (q, *J* = 8.3, Hz, 1H, CH of cyclooctadienyl), 3.80–3.66 (m, 1H, PCH₂), 3.64–3.56 (m, 1H, RuCHCH), 3.37 (d, *J* = 6.8 Hz, 1H, RuCH), 3.26 (s, 3H, OCH₃), 3.24 (s, 3H, OCH₃), 3.14 (s, 3H, OCH₃), 3.00 (s, 3H, OCH₃), 2.93–2.74 (m, 2H, CH of cyclooctadienyl and PCH₂), 2.61–2.32 (m, 1H, PCH₂), 2.26 (s, 3H, NCH₃), 2.24–2.16 (m, 1H, CH of cyclooctadienyl), 1.70–1.44 (m, 2H, CH₂ of cyclooctadienyl), 1.15–1.07 (m, 1H, CH₂ of cyclooctadienyl), 0.92–0.76 (m, 1H, PCH₂), 0.61 (dt, *J* = 4.8, 13.8 Hz, 1H, CH₂ of cyclooctadienyl). ¹³C NMR (75 MHz, CD₂Cl₂): δ 193.0 (C=O), 182.6 (C=O), 160.3–110.3 (C_{Ar}), 98.1 (CH of cyclooctadienyl), 96.2 (CH of cyclooctadienyl), 89.1 (CH of cyclooctadienyl), 77.9 (d, *J*_{CP} = 18.1 Hz, CH of cyclooctadienyl), 64.7 (d, *J*_{CP} = 8.1 Hz, RuCH), 55.2 (OCH₃), 55.2 (OCH₃), 55.0 (OCH₃), 54.9 (OCH₃), 50.4 (d, *J*_{CP} = 34.8 Hz, CH of cyclooctadienyl), 40.2 (CH of cyclooctadienyl), 28.2 (RuCHCH), 26.3 (d, *J*_{CP} = 15.6 Hz, PCH₂), 25.9 (d, *J*_{CP} = 10.0 Hz, PCH₂), 25.2 (CH₂ of cyclooctadienyl), 24.9 (CH₂ of cyclooctadienyl), 24.9 (NCH₃). HR-MS (FAB-*m*NBA): calcd for C₄₃H₄₇NO₆P₂Ru 837.1922, found 837.1947 (M⁺).

Synthesis of Complexes 12a and 12b. Complexes **12a** and **12b** were synthesized in a similar manner. The following procedure for **12a** is representative.

Complex 12a. Into a 20 mL, two-necked Pyrex flask equipped with a stirring bar and a reflux condenser was placed complex **4d** (244 mg, 0.50 mmol) under a CO atmosphere. Toluene (10 mL) was then added, and the suspension was magnetically stirred at 120 °C for 3 h. After removal of the solvent, Et₂O (2.0 mL) and hexane (2.0 mL) were added to the residue, and the resulting solid was collected by a G4-glass filter, washed (4 × 2 mL of hexane), and dried under vacuum to give complex **12a** (174 mg, 76%) as a pale yellow solid. Mp: 156–159 °C (dec). IR (KBr disk): 2085, 2016, 2001, 1746, 1681, 1378, 1165, 1016 cm⁻¹. ¹H NMR (400 MHz, CD₂Cl₂): δ 7.45 (dt, *J* = 1.6, 6.7 Hz, 2H, H_{Ar}), 7.36 (tt, *J* = 1.6, 7.3 Hz, 1H, H_{Ar}), 7.31 (dd, *J* = 1.5, 7.3 Hz, 2H, H_{Ar}), 6.13 (dd, *J* = 10.5, 3.2 Hz, 1H, free =CH), 5.71 (dq, *J* = 0.8, 8.8 Hz, 1H, free =CH), 5.03 (br d, *J* = 7.3 Hz, 1H, CH of cyclooctadienyl), 4.94 (t, *J* = 8.3 Hz, 1H), 4.90 (dt, *J* = 1.6, 8.3 Hz, 1H, CH of cyclooctadienyl), 3.52–3.42 (m, 1H, CH of cyclooctadienyl), 3.02 (dd, *J* = 8.8, 3.6 Hz, 1H, RuCHCH), 2.66–2.55 (m, 1H, CH₂ of cyclooctadienyl), 2.34 (d, *J* = 8.8 Hz, 1H, RuCH), 2.32–2.26 (m, 1H, CH₂ of cyclooctadienyl), 1.82 (ddt, *J* = 14.0, 6.2, 2.0 Hz, 1H, CH₂ of cyclooctadienyl), 1.63 (dddd, *J* = 14.2, 12.7, 5.4, 2.0 Hz, 1H, CH₂ of cyclooctadienyl). ¹³C NMR (100 MHz, CD₂Cl₂): δ 197.9 (RuCO), 194.7 (RuCO), 188.8 (C=O), 185.7 (RuCO), 180.7 (C=O), 133.4 (free C=C), 132.4 (free C=C), 129.4 (C_{Ar}), 128.9 (2C, C_{Ar}), 127.9 (C_{Ar}), 126.9 (2C, C_{Ar}), 97.8 (CH of cyclooctadienyl), 79.7 (CH of cyclooctadienyl), 66.1 (CH of cyclooctadienyl), 63.4 (RuCHCH), 42.0 (CH of cyclooctadienyl), 35.3 (RuCH), 32.7 (CH₂ of cyclooctadienyl), 25.7 (CH₂ of cyclooctadienyl). HR-MS (FAB-*m*NBA): calcd for C₂₁H₁₈NO₅Ru 466.0228, found 466.0237 (M⁺ + H).

Complex 12b: pale yellow solid, mp 154–156 °C (dec). IR (KBr disk): 2089, 2018, 2010, 1747, 1684, 1512, 1384, 1249, 1165, 1101, 1028 cm⁻¹. ¹H NMR (400 MHz, CDCl₃): δ 7.21 (d, *J* = 8.8 Hz,

Table 2. Summary of Crystal Data, Collection Data, and Refinement of 4e and 11a

	4e	11a
formula	C ₂₇ H ₃₁ NO ₃ Ru	C ₄₄ H ₄₁ NO ₂ P ₂ Ru·CH ₂ Cl ₂
fw	518.62	863.76
cryst color	yellow	yellow
habit	prism	block
cryst size, mm	0.20 × 0.10 × 0.10	0.15 × 0.15 × 0.10
cryst syst	orthorhombic	triclinic
space group	<i>Pbca</i> (#61)	<i>P1</i> (#2)
<i>a</i> , Å	15.4164(9)	10.4811(13)
<i>b</i> , Å	13.1723(7)	15.523(3)
<i>c</i> , Å	21.0485(4)	24.0006(12)
α, deg	90	90.466(7)
β, deg	90	91.225(3)
γ, deg	90	93.021(8)
<i>V</i> , Å ³	4274.3(3)	3898.3(9)
<i>Z</i>	8	4
<i>D</i> (calcd), g cm ⁻³	1.612	1.472
data collection	-80	-130
temp, °C		
μ(Mo Kα), cm ⁻¹	7.651	6.612
2θ _{max} , deg	55.0	54.8
no. of measd reflns	23 658	28 588
no. of unique reflns	4862 (<i>R</i> _{int} = 0.148)	15 192 (<i>R</i> _{int} = 0.069)
no. of obsd reflns (<i>I</i> > 2σ(<i>I</i>))	2723	10 070
no. of variables	320	1041
<i>R</i> ₁ ^a (<i>I</i> > 2σ(<i>I</i>))	0.042	0.073
<i>wR</i> ₂ ^a (<i>I</i> > 2σ(<i>I</i>))	0.066	0.131
<i>R</i> ₁ ^a (all data)	0.107	0.120
<i>wR</i> ₂ ^a (all data)	0.113	0.150
GOF	1.047	0.978

$$^a R_1 = \sum ||F_o| - |F_c|| / \sum |F_o|; wR_2 = [\sum (w(F_o^2 - F_c^2)^2) / \sum w(F_o^2)]^{1/2}.$$

2H, H_{Ar}), 6.96 (d, *J* = 8.8 Hz, 2H, H_{Ar}), 6.12 (dd, *J* = 10.3, 2.9 Hz, 1H, free =CH), 5.70 (dt, *J* = 10.4, 8.0 Hz, 1H, free =CH), 5.02 (br d, *J* = 6.4 Hz, 1H, CH of cyclooctadienyl), 4.93 (t, *J* = 8.4 Hz, 1H, CH of cyclooctadienyl), 4.89 (t, *J* = 8.4 Hz, 1H, CH of cyclooctadienyl), 3.82 (s, 3H, OCH₃), 3.44 (br s, 1H, CH of cyclooctadienyl), 3.00 (dd, *J* = 8.8, 3.6 Hz, 1H, RuCHCH), 2.66–2.53 (m, 1H, CH₂ of cyclooctadienyl), 2.33 (d, *J* = 8.8 Hz, 1H, RuCH), 2.30–2.26 (m, 1H, CH₂ of cyclooctadienyl), 1.85–1.78 (m, 1H, CH₂ of cyclooctadienyl), 1.63 (dt, *J* = 5.2, 12.4 Hz, 1H, CH₂ of cyclooctadienyl). ¹³C NMR (100 MHz, CDCl₃): δ 198.0 (RuCO), 194.8 (RuCO), 188.8 (C=O), 185.9 (RuCO), 180.9 (C=O), 159.1 (C_{Ar}), 132.4 (free C=C), 129.3 (free C=C), 128.0 (2C, C_{Ar}), 126.1 (C_{Ar}), 114.2 (2C, C_{Ar}), 97.8 (CH of cyclooctadienyl), 79.7 (CH of cyclooctadienyl), 66.0 (CH of cyclooctadienyl), 63.3 (RuCHCH), 55.8 (OCH₃), 42.0 (CH of cyclooctadienyl), 35.2 (RuCH), 32.7 (CH of cyclooctadienyl), 25.7 (CH₂ of cyclooctadienyl). Anal. Calcd for C₂₂H₁₉NO₆Ru: C, 53.44; H, 3.87; N, 2.83. Found: C, 53.44; H, 3.87; N, 2.99.

Crystallographic Study of Complexes 4e and 11a. Crystals that were stable for X-ray diffraction measurements and were obtained by recrystallization from CHCl₃/pentane for **4e** and CH₂-Cl₂/pentane for **11a** were mounted on glass fibers. The diffraction data were collected with a Rigaku RAPID imaging plate area detector, using graphite-monochromated Mo Kα radiation (λ = 0.71069 Å) with the oscillation technique. Crystal data and experimental details are listed in Table 2. All structures were solved by a combination of direct methods and Fourier techniques. Non-hydrogen atoms were anisotropically refined by full-matrix least squares calculations. Refinements were continued until all shifts were smaller than one-tenth of the standard deviations of the parameters involved. Atomic scattering factors and anomalous dispersion terms were taken from the International Tables for X-ray

Crystallography.³⁵ All calculations were carried out with a Japan SGI workstation computer using the CrystalStructure crystallographic software package.^{36,37}

Theoretical Calculations. To consistently compare the single-point energies of model complexes, calculations were carried out using density functional theory (DFT)-optimized geometries. Calculations were performed using the Gaussian 03 RevB.04³⁸ implementation of B3LYP [Becke three-parameter exchange functional (B3)³⁹ and the Lee–Yang–Parr correlation functional (LYP)⁴⁰] on Intel PIV computers at Kyoto University. The basis set consisted of the combination of the Stuttgart–Dresden–Bonn energy-consistent pseudopotential (SDD)⁴¹ for Ru and the 6-31G-(d,p) basis set for all other atoms. No constraints were imposed for any of the systems. Frequency calculations on optimized species established that the energy minima possessed only real frequencies and the transition states possessed a single imaginary frequency. Zero-point energy and thermodynamic functions were computed at standard temperature (298.15 K) and pressure (1 atm). Spatial plots of the optimized geometries were obtained from Gaussian 03 output using Cambridge Soft Corporation's Chem 3D Pro v4.0.

Acknowledgment. This work was supported in part by Grants-in-Aid for Scientific Research (A), (B), Scientific Research on Priority Areas, and the 21st century COE program, COE for a United Approach to New Materials Science, from the Japan Society for the Promotion of Science and the Ministry of Education, Culture, Sports, Science and Technology, Japan. T.K. acknowledges financial support from the Sumitomo Foundation and the Japan Chemical Innovation Institute. We thank Dr. M. Shiro (Rigaku Corp.) for supporting our X-ray crystallography. This research (project) was partly conducted in the Advanced Research Institute of Environmental Material Control Engineering, Katsura-Int'ech Center, Graduate School of Engineering, Kyoto University.

Supporting Information Available: X-ray crystallographic files (CIF) for complexes **4e** and **11a** and results of the theoretical calculations. This material is available free of charge via the Internet at <http://pubs.acs.org>.

OM060242T

(35) Ibers, J. A.; Hamilton, W. C., Eds. *International Tables for X-ray Crystallography*; Kynoch Press: Birmingham, UK, 1974; Vol. IV.

(36) *CrystalStructure 3.7.0, Crystal Structure Analysis Package*; Rigaku and MSC, 2005.

(37) Watkin, D. J.; Prout, C. K.; Carruthers, J. R.; Betteridge, P. W. *CRYSTALS Issue 10*; Chemical Crystallography Laboratory: Oxford, UK, 1996.

(38) Frisch, M. J.; Trucks, G. W.; Schlegel, H. B.; Scuseria, G. E.; Robb, M. A.; Cheeseman, J. R.; Montgomery, J. A., Jr.; Vreven, T.; Kudin, K. N.; Burant, J. C.; Millam, J. M.; Iyengar, S. S.; Tomasi, J.; Barone, V.; Mennucci, B.; Cossi, M.; Scalmani, G.; Rega, N.; Petersson, G. A.; Nakatsuji, H.; Hada, M.; Ehara, M.; Toyota, K.; Fukuda, R.; Hasegawa, J.; Ishida, M.; Nakajima, T.; Honda, Y.; Kitao, O.; Nakai, H.; Klene, M.; Li, X.; Knox, J. E.; Hratchian, H. P.; Cross, J. B.; Adamo, C.; Jaramillo, J.; Gomperts, R.; Stratmann, R. E.; Yazyev, O.; Austin, A. J.; Cammi, R.; Pomelli, C.; Ochterski, J. W.; Ayala, P. Y.; Morokuma, K.; Voth, G. A.; Salvador, P.; Dannenberg, J. J.; Zakrzewski, V. G.; Dapprich, S.; Daniels, A. D.; Strain, M. C.; Farkas, O.; Malick, D. K.; Rabuck, A. D.; Raghavachari, K.; Foresman, J. B.; Ortiz, J. V.; Cui, Q.; Baboul, A. G.; Clifford, S.; Cioslowski, J.; Stefanov, B. B.; Liu, G.; Liashenko, A.; Piskorz, P.; Komaromi, I.; Martin, R. L.; Fox, D. J.; Keith, T.; Al-Laham, M. A.; Peng, C. Y.; Nanayakkara, A.; Challacombe, M.; Gill, P. M. W.; Johnson, B.; Chen, W.; Wong, M. W.; Gonzalez, C.; Pople, J. A. *Gaussian 03, revision B.04*; Gaussian, Inc.: Pittsburgh, PA, 2003.

(39) Becke, A. D. *J. Chem. Phys.* **1993**, *98*, 5648.

(40) Lee, C.; Yang, W.; Parr, R. G. *Phys. Rev. B* **1988**, *37*, 785.

(41) Dolg, M. *Modern Methods and Algorithms of Quantum Chemistry*; Grotendorst, J., Ed.; John von Neumann Institute for Computing: Zürich, 2000, Vol. 1, pp 479–508.